수의학석사 학위논문

Trivalent iron-induced conversion of prion protein to a proteinase K resistant form in vesicular trafficking

Fe (III)에 의한 PrP^{res} 형성

2012년 8월

서울대학교 대학원

수의학과 인수공통동물질병학 전공

최 보 란

Trivalent iron-induced conversion of prion protein to a proteinase K resistant form in vesicular trafficking

Fe (III)에 의한 PrP^{res} 형성

지도교수 우 희 종

이 논문을 수의학석사학위논문으로 제출함
2012 년 4 월

서울대학교 대학원

수의학과 인수공통동물질병학 전공

최 보 란

최보란의 석사학위논문을 인준함
2012 년 6 월

위 원 장 박 재 학 (인)
부위원장 우 희 종 (인)
위 원 이 장 헌 (인)

Abstract

Trivalent iron-induced conversion of prion protein to a proteinase K resistant form in vesicular trafficking

Bo-Ran Choi
Department of Veterinary Immunology
The Graduate School
Seoul National University

Prion disorders belong to the group of neurodegenerative diseases involving protein misfolding. Prion protein (PrP) aggregation and neurotoxicity are believed to result from the accumulation of infectious PrP (PrP^{Sc}), a particular misfolded form of the normal PrP (PrP^{C}). The biochemical features of PrP^{Sc} are resistance to proteinase K (PK) digestion and detergent insolubility. The physiological roles of PrP^{C} are yet to be defined; however, some studies have shown that PrP^{C} may be involved in metal ion homeostasis. In diseased brains, iron levels are increased, which is possible because of the coaggregation of PrP with ferritin. Although iron is known to be involved in the generation of abnormal PrP, little is known about the contribution of oxidation state-

dependent iron to PrP conversion and the conversion mechanism in neural cells. In this study, murine PrP^{C}-deficient cells (HpL3-4) were exposed to divalent [Fe (II)] or trivalent [Fe (III)] iron and then treated with exogenous recombinant PrP (rPrP). After the internalization of rPrP by the cells, we analyzed the accumulation of intracellular rPrP and its biochemical properties in combination with PK resistance and detergent insolubility. U18666A and NH_4Cl were used to inhibit vesicular trafficking and endolysosomal acidification, respectively. We found that Fe (III) induced an increase of internalized rPrP in a time- and dose-dependent manner. Moreover, the accumulated rPrP was converted to detergent-insoluble and PK-resistant PrP (PrP^{res}) in part. The generation of PrP^{res} was hindered by U18666A, but not by NH_4Cl, indicating that Fe (III)-mediated PrP^{res} conversion possibly occurred during endosomal vesicular trafficking and not in the acidic environment of lysosomes. These results suggest that Fe (III), and not Fe (II), has a role in the generation of PrP^{res} during endosomal vesicular trafficking.

Key words

iron, recombinant PrP, conversion, PrP^{res}, vesicular trafficking, lysosomes,

Student Number: 2009-21645

Contents

List of Figures

I. INTRODUCTION

Fatal neurodegenerative prion disorders occur in many vertebrates including human, cattle, and small ruminants. These disorders belong to the family of protein misfolding diseases including Alzheimer's disease, Huntington's disease, and Parkinson's disease. The central event in all prion disorders is the conversion of PrP to a beta-sheet rich form (PrP scrapie; PrP^{Sc}) from an alpha-helix rich form of PrP (cellular PrP; PrP^{C}**).** The generation of PrP^{Sc} has been observed in exogenous prion sources, including scrapie in sheep, bovine spongiform encephalopathy in cattle, chronic wasting disease in deer and elk; it has also been observed to result from the pathological mutations in the gene for PrP, or from stochastic misfolding of PrP^{C} in sporadic Creutzfeldt-Jacob disease (Collinge, 2001). Resistance to limited proteolysis and detergent insolubility are biochemical features of the abnormal PrP distinguished from the normal PrP.

Even though PrP aggregation and neurotoxicity are believed to result from the accumulation of PrP^{Sc}, these main pathologies might be caused not only by PrP^{Sc} but also by other elements or factors of prion pathogenesis (Das et al., 2010; Zhou et al., 2012). In diseased brains, imbalance in brain metal homeostasis and associated oxidative stress have been observed (Singh et al., 2010; Rana et al., 2009; Fernaeus and Land, 2005). Proposed hypotheses include a functional role of PrP^{C} in homeostasis of iron and copper, and loss of this function due to aggregation with the disease-associated PrP^{Sc} form

probably causing an imbalance of metals in the brain. Other views suggest that PrP^{Sc} acquires a toxic function due to sequestration of PrP^{C}-associated metals within the aggregates, resulting in the generation of redox-active PrP^{Sc} complexes (Singh et al., 2009; Pauly and Harris, 1998; Brown et al. 2000). In support of these hypotheses, iron content is observed to increase in the cerebral cortex, striatum, and brain stem of scrapie-infected mice (Singh et al., 2009; Kim et al., 2007); however, copper content is observed to decrease (Thackray et al., 2002). Increased iron induces oxidative stress-associated neurotoxicity and aggravated impairment of antioxidant activities in prion-infected cells and animals (Fernaeus, 2005; Wong, 2001). Recently, several investigations have addressed the relationship between redox-iron and PrP (Kim et al., 2000; Singh et al., 2009). Iron overload induced the aggregation of PrP^{C} and rendered PrP resistant to proteinase K (PK) digestion (Basu et al., 2007; Singh et al., 2009). Moreover, neurotoxicity associated with aggregates of PrP and iron has been studied in PrP^{C} over-expressing neuroblastoma cells (Das et al., 2010; Basu et al., 2007; Singh et al., 2009). However, the relative contribution of the 2 oxidative states of iron, divalent [Fe (II)] or trivalent [Fe (III)], in the generation of abnormal PrP isoforms has not been investigated. In addition, mechanisms for iron-mediated PrP transformation remain to be determined.

Establishment of an experimental cell model in which prion conversion takes place in the absence of interference of endogenous PrP^{C} would provide a tractable system for evaluating PrP alteration processes. Even though intensive efforts have been focused on defining the mechanisms of PrP^{Sc}

formation, the cell biology of prion conversion and its cellular effect(s) are not fully understood. Approaches using cell-free conditions have attempted to study factors associated with PrP aggregation and PK resistance (Jackson et al., 1999; Martins et al., 2006; Qin et al., 2000), but by their nature lack biological context. Cell lines that are susceptible to prion infection have been used to delineate the conversion processes but are limited because PrP^{Sc} is immunologically indistinguishable from PrP^{C} (Alais et al., 2008; Marijanovic et al., 2009). Moreover, cytotoxic effects specifically associated with the intracellular accumulation of abnormal isoforms are poorly defined due to the additional effects caused by the loss of PrP^{C} normal function (Westergard et al., 2007; Das et al., 2010). Therefore, an experimental cell model that induces intracellular PrP conversion without interference from endogenous PrP^{C} would be useful to understand the conversion process and to evaluate the cytotoxic effect of converted PrP.

In this study, cells devoid of endogenous PrP^{C} were overloaded with iron and treated with recombinant bovine prion protein (rPrP). We exploited iron to induce intracellular PrP conversion over copper because of its pathological implications in prion diseases. From our results, Fe (III), but not Fe (II), induced an accumulation of internalized rPrP and converted PrP to a PK-resistant form (PrP^{res}). Reactive oxygen species (ROS) were partly involved in the generation of Fe (III)-mediated PrP^{res}; however, our data suggest additional endogenous factors remain to be identified. Moreover, endosomal trafficking and not the acidic environment of lysosomes appears to be a critical process for Fe (III)-induced PrP^{res} generation.

II. MATERIALS AND METHODS

Reagents

The PrP-deficient HpL3-4 cell line (Kuwahara et al. 1999) was kindly provided by Prof. Yong-Sun Kim (Hallym University, South Korea) under the permission of Prof. Takashi Onodera (University of Tokyo, Japan). The neuronal cell line was maintained in complete medium, the high glucose Dulbecco's modified Eagle's medium (DMEM) containing 10% heat-inactivated fetal bovine serum (FBS) at 37°C with 5% CO_2. DMEM and FBS were purchased from Invitrogen Life Technologies (Grand Island, NY, USA) and Hyclone (Logan, UT, USA), respectively. Mouse anti-prion protein monoclonal antibody against amino acid 108-119 in prion, 1E4, was purchased from Abcam (Cambridge, UK). Rabbit anti-lamin A/C monoclonal antibody was obtained from Santa Cruz Biotechnology (Santa Cruz, C.A, USA), and anti-β-actin was obtained from Cell Signaling Technology (Beverly, MA, USA). For HRP-conjugated secondary antibodies, anti-mouse IgG antibody was obtained from Cell Signaling Technology (Beverly, MA, USA), anti-goat IgG antibody was purchased from Santa Cruz Biotechnology (Santa Cruz, C.A, USA), and anti-rabbit IgG was from Sigma (Sigma-Aldrich, MO, USA). Protease K was purchased from Invitrogen Life Technologies (Grand Island, NY, USA). U18666A from Enzo Life Sciences (Farmingdale, NY, USA) was reconstructed according to

the manufacturer's instructions. The BCA protein assay kit was purchased from Pierce Chemical (Rockford. IL, USA). Unless indicated otherwise, all the chemicals including ferrous chloride ($FeCl_2$) and ferric ammonium citrate (FAC) were purchased from Sigma-Aldrich Co. (St. Louis, MO, USA).

Generation of recombinant proteins

rPrP cloned in a pET23 vector (Novagen, Madison, WI, USA) was expressed in *Escherichia coli* BL21 (DE3) after induction with isopropyl-β-D-thiogalactopyranoside (IPTG, 1 mM) for 14 h. The cells were re-suspended in cold PBS with 5 mM ethylenediaminetetraacetic acid (EDTA) and protease inhibitor cocktail and then sonicated. Inclusion bodies were collected by centrifugation at 100,000 × *g* for 30 min and solubilized with buffer A (20 mM sodium phosphate, pH 7.4; 6 M guanidine hydrochloride [GdnHCl]; 20 mM imidazole; 0.5 M NaCl). After brief sonication, the solubilized proteins were collected by centrifugation at 100,000 × *g* for 30 min. Cleared lysates were loaded onto HiTrap Chelating HP column (GE Healthcare, WI, USA), and rPrP was eluted using buffer B (20 mM sodium phosphate, pH 7.4, 6 M GdnHCl, 0.5 M imidazole, 0.5 M NaCl). Fractions were dialyzed against 50 mM sodium acetate, pH 5.0, containing 5% glycerol and then re-dialyzed against 20 mM HEPES at pH 7.4.

Recombinant human galectin-3 (rGal-3) cloned in a pET21a vector

(Novagen, Madison, WI, USA) was expressed in *E. coli* BL21 (DE3) after induction with 1 mM IPTG for 6 h. The cells were lysed by performing sonication, and the lysates were clarified at 80,000 × *g* for 20 min at 4°C. rGal-3 was purified from the lysates by performing affinity chromatography with asialofetuin-Sepharose 4B and washed with 100 mM sodium phosphate, pH 7.2, containing 150 mM NaCl followed by PBS containing 2 mM dithiothreitol (DTT). Competitive elution was performed with 0.4 M lactose in PBS containing 2 mM DTT. The eluted proteins were dialyzed against PBS and redialyzed against 20 mM HEPES at pH 7.4.

Treatment of cells with iron and rPrP

The cells were plated with a density at 0.4×10^5 cells/mL. After 4 h of stabilization, the cells were exposed to either 0.3 mM $FeCl_2$ designated as Fe (II) or 0.6 mM FAC as Fe (III) for 24 h. Then 0.6 μM rPrP (about 25 μg/mL) were added to the media and incubated for another 24 h. Mock-exposed cells treated with rPrP were used as the control. For analyzing the effects of other trivalent metal ion exposures, 0.6 mM aluminum chloride [Al (III)] and chromium chloride [Cr (III)] were used. To assess ROS involvement in the generation of PrP^{res}, dimethyl sulfoxide (DMSO) at the indicated concentrations was added to the cells 30 min prior to iron exposure, and then rPrP treatment was performed. In an attempt to assess the intracellular conversion process, U18666A and ammonium chloride (NH_4Cl) were used. U18666A was constructed in the complete medium at 3 μM concentration.

Cells exposed to Fe (II) or Fe (III) were subsequently treated with the drug. After 24 h of incubation, rPrP was added and incubated for a further 24 h. For NH_4Cl treatment, 20 mM NH_4Cl was added 30 min prior to the rPrP treatment. To analyze changes in the level of PrP^{res}, cell lysates were either treated with PK at 5 μg/mL and subjected to immunoblotting or were left untreated.

Whole cell lysates preparation

After trypsinization, the cells were washed with PBS 3 times to exclude contamination with rPrP from media. The collected cells were lysed in buffer A (20 mM Tris-HCl, pH 7.4, 150 mM NaCl, 2 mM EDTA, 0.25% sodium dodecyl sulfate (SDS), 2% NP-40, 1% sodium deoxycholate, protease inhibitor cocktail, PMSF) for 30 min at 4°C. After a brief centrifugation, the supernatant was collected, and total protein concentration was measured using the BCA protein assay kit.

Proteinase K treatment

After metal exposure and rPrP treatment, the PBS-washed cells were lysed in buffer A without protease inhibitors. Digestion was performed by treating the protein of each sample (1 mg/mL) with 5 μg/mL concentration of PK at 37°C for 30 min. The reaction was arrested by adding 1 mM PMSF.

Detergent insolubility

After washing with PBS, the cells were collected in lysis buffer A, and large debris were removed by centrifugation at 350 × *g* for 5 min. Supernatants were subjected to centrifugation at 16,000 × *g* for 45 min. Protein concentration was measured by performing the BCA protein assay. Samples of the insoluble fraction from re-suspended pellets and of the soluble fraction from supernatants were prepared.

Assessment of cytotoxicity

Cytotoxicity was determined using the WST-8 assay using the Cell Counting Kit-8 (CCK-8; Dojindo Molecular Technologies, Kumamoto, Japan). Cells were exposed to $FeCl_2$ or FAC at various concentrations, and then incubated with 10 μL of WST-8 for another 4 h. The absorbance was measured at 450 nm, and the results were expressed as means +/- standard deviation (STDV).

Immunoblotting

Sample proteins subjected to 15% sodium dodesyl sulfate polyacrylamide gel electrophoresis (SDS-PAGE) were transferred onto polyvinylidene difluoride (PVDF) membranes (Millipore; Immobilon-P membranes). The membranes were blocked using 5% nonfat dry milk in TBS-Tween for 2 h at

room temperature. Membranes were probed overnight by using the primary anti-PrP antibody 1E4, anti-galectin-3 antibody m3/38 (purified in our laboratory), anti-lamin A/C antibody, or β–actin antibody, followed by treatment with appropriate secondary antibodies. The blots were developed by using enhanced chemiluminescence (GE Healthcare, Waukesha, WI, USA). Relative intensity of the proteins was analyzed using ImageJ analysis (Window version; National Institutes of Health, Bethesda, MD, USA).

Statistical analysis

All the experiments were repeated at least 3 times. The results are expressed as mean +/- STDV. Statistical analysis was performed by Tukey's test for comparing multiple groups using the SPSS software (SPSS, Chicago, USA). Differences were considered significant at a p value of <0.01.

II. RESULTS

Cytotoxicity of iron in HpL3-4 cells

Iron exposure to HpL3-4 cells exhibited marginal cytotoxicity. The cytotoxicity of the 2 states of iron over a range of concentrations (0.3-2.4 mM for $FeCl_2$ and FAC) was examined to select an optimal concentration of metal exposure for investigating metal-mediated intracellular conversion of PrP. Perturbations of various metals including iron and copper have been observed in prion diseases. Iron was chosen for the study due to its high redox-active property and physiological interaction with PrP (Pauly and Harris, 1998; Brown and Harris, 2003; Singh et al., 2009) but also increases of the 2 transitional states of iron as well as total iron in prion disease-affected human and animal brains (Singh et al., 2009; Kim et al., 2000). For iron exposure, 0.3 mM $FeCl_2$ is an optimal concentration for generation of PrP^{Sc}-like aggregates in endogenous PrP^{C}-overexpressing human neuroblastoma cells (PrP^{C} cells) (Basu et al., 2007). This treatment simulates in vivo conditions of oxidative stress, for which an active fragment of protein kinase C (PKC) δ is considered to be a positive biomarker (Kaul et al., 2003). The cytotoxicity of 0.3 mM $FeCl_2$ exposure in HpL3-4 cells for 48 h produced less than 5% reduction in cell viability, unlike that observed in the control (Fig. 1). The cytotoxicity of FAC showed no significant reduction in cell viability at the concentration of up to 0.6 mM, and was

always lower than that observed with $FeCl_2$ at the same concentrations.

Accumulation of internalized rPrP after Fe (III) exposure

To investigate the effect of the 2 states of iron on intracellular PrP accumulation and conversion to a PrP^{Sc}-like isoform, exogenous rPrP was added to the cells after metal exposure. Preliminary experiments confirmed that the treatment of histidine-tagged rPrP at 0.6 μM did not affect cell viability (data not shown). Cells were exposed to $FeCl_2$ or FAC over a range of concentrations from 0.3 to 1.2 mM. After 24 h of iron exposure, 0.6 μM rPrP was additionally added to the media, and the cells were incubated for another 24 h. The level of internalized rPrP from whole cell lysates was detected using 1E4 antibody, which recognizes amino acids 108-119 of bovine PrP including the N-terminal part of the PK-resistant PrP^{27-30} fragment. The levels of internalized rPrP were proportional to the iron concentration (Fig. 2). Interestingly, the amount of rPrP from the Fe (III)-exposed cells was considerably higher than the Fe (II)-exposed cells. Fe (III) dramatically induced a 13-fold increase in the level of rPrP, unlike that observed in the mock-exposed control (Fig. 3-A, lane 5, and Fig. 3-B); however, cells with Fe (II) exposure displayed a marginal increase compared to the controls (Fig. 3-A, lane 4, and Fig. 3-B). No signals were detected from the cells without rPrP treatment (Fig. 3-A, lane 2), demonstrating a specific detection of internalized rPrP with the 1E4 antibody.

Incubation of cells with rPrP for 4, 8, 16, and 24 h showed that the accumulation was time-dependent. In the cells exposed to Fe (III), the level of rPrP increased over time (Fig. 4). It was low at early timepoints during the incubation (4 h, lane 9), but increased dramatically at later times (8, 16 and 24 h, lane 10–12). Although cells exposed to Fe (II) displayed an increase in rPrP until 16 h of incubation, the increase was marginal and eventually returned to the control levels (lane 5–8).

It was uncertain whether the increase in rPrP was specific to Fe (III) or whether any trivalent cation would elicit a similar effect. To determine this, cells were exposed to other trivalent metal ions including Al (III) and Cr (III). However, neither Al (III) nor Cr (III) exposure induced the accumulation of rPrP (Fig. 5).

To verify whether the Fe (III)-mediated increase in rPrP was specific to that particular protein, or was a general phenomenon applicable to other exogenous proteins, we treated cells with 0.6 μM of rGal-3, which has a similar molecular weight (29 kDa) to rPrP. The level of internalized rGal-3 in Fe (III)-exposed cells was similar to that in the control cells (Fig. 6). Endogenous galectin-3 in HpL3-4 cells had a slightly higher molecular weight (ca.30 kDa) (Henderson, 2006) and was expressed at comparable levels in the control and Fe (III)-exposed cells.

Detergent insolubility of internalized rPrP

A detergent solubility assay is commonly used to distinguish PrP^{Sc}-like characteristics from PrP^{C}. To examine the solubility of internalized rPrP, cells were lysed in a buffer containing the ionic denaturant SDS at a concentration of 0.25%. Equal amounts of the proteins were fractionated into soluble and insoluble compartments, and rPrP from each fraction was detected. rPrP was present mainly in the insoluble fraction, while lamin A/C, a nuclear membrane protein, was found in the soluble fraction regardless of metal exposure (Fig. 7). Endogenous PrP^{C} is known to be soluble (Thellung et al., 2011), whereas internalized rPrP was observed to be insoluble.

Intracellular conversion to PrP^{res} with Fe (III)

Resistance to PK treatment is considered a hallmark of PrP^{C}-to-PrP^{Sc} conversion. To assess whether internalized rPrP subjected to iron exposure showed PrP^{Sc}-like characteristics, resistance against PK digestion was analyzed (Fig 8). Cells were treated with lysis buffer without protease inhibitors and then incubated with PK (0, 1, 5, 10 μg/mL). rPrP from Fe (III)-exposed cells displayed partial PK resistance, designated as PrP^{res} (Fig. 8, lane 9–12). Upon increasing concentrations of PK, intact rPrP (25 kDa) underwent digestion and generated a PK-resistant fragment (16 kDa). On the contrary, rPrP from the control and Fe (II)-exposed cells was completely degraded at a minimal concentration of 1 μg/mL. To define whether a direct reaction between rPrP and Fe (III) might have induced PrP^{res} formation, 0.6 μM rPrP in HEPES buffer was exposed to iron under cell-free conditions

(Fig. 9). Immunoblots revealed that this simple reaction failed to render rPrP resistance against PK digestion. These data indicate that Fe (III)-mediated conversion to PrP^{res} occurs in a complex cellular milieu.

Involvement of ROS in the generation of PrP^{res} with Fe (III)

Since iron is a known to be a redox-active metal ion, and iron-associated oxidative stress has been implicated in prion pathologies (Milhavet et al., 2000; Petersen et al., 2005), the effect of DMSO on the formation of PrP^{res} was examined. DMSO is a ROS scavenger and reduces hydrogen peroxide-induced intracellular ROS production (Watt et al., 2005). When the cells were incubated with DMSO (0.5 and 1 %), there was a dose-dependent reduction of PrP^{res} (Fig. 10).

Fe (III)-mediated conversion in vesicular trafficking

To examine an intracellular process in which PrP^{res} was formed, we used U18666A, which is known to effectively inhibit vesicular trafficking from early endosomes (EE) to late endosomes (LE), LE to lysosomes (LY), and LY to plasma membrane or endoplasmic reticular, by the induction of cholesterol accumulation in LE and LY. These effects of U18666A ultimately prevent protein degradation (Cenedella, 2009; Mayran et al., 2003; Kobayashi et al., 1999). Mock or 3 μM U18666A was added to the media

after the cells had been exposed to iron. Under the drug treatment, PrP^{res} disappeared, although the high level of rPrP were still detected in the Fe (III)-exposed cells (Fig. 11). Next, the involvement of the acidic environment of LY in the formation of PrP^{res} was examined using NH_4Cl. This compound is an inhibitor of endolysosomal acidification and impairs the lysosomal degradation system (Misinzo, 2008). Iron-exposed cells were pretreated with 20 mM of NH_4Cl before rPrP addition. Endolysosomal acidification inhibition had a negligible effect on the reduction of PrP^{res} (Fig. 12). Noticeably, following impairment of the lysosomal degradation system, high levels of rPrP in both control and Fe (II)-exposed cells were observed; however, the prion was completely digested by PK treatment in both the cases.

IV. DISCUSSION

In this study, internalized rPrP was converted into PrP^{res} by Fe (III) during vesicular trafficking in the cells devoid of endogenous PrP^{C}. The accumulation and conversion of rPrP was specifically induced by Fe (III) but not by Fe (II), despite previous assumptions that both cations participated equally in prion diseases (Fig. 3 and 8). Notably, the discrepancy in the level of intracellular rPrP was due to the acquisition of resistance to cellular degradation, rather than to a differential cellular uptake of rPrP. Moreover, other trivalent metal ions such as Al (III) and Cr (III) failed to induce rPrP accumulation, and other exogenous protein such as rGal-3 did not accumulate after by Fe (III) treatment (Fig. 5 and 6); these data indicate a specific reaction between Fe (III) and rPrP.

From previous studies involving prion-infected cells and brains (Singh et al., 2009; Fernaeus and Land, 2005; Petersen et al., 2005), iron has been implicated in prion pathology; however, the level of contribution of each oxidation state of iron to prion conversion has not been fully investigated. Studies of Singh and colleagues reported that $FeCl_2$ and FAC induced a prion conformational change into detergent-insoluble and/or PK-resistant isoforms when exposed to cells that overexpress endogenous PrP^{C} (Das et al., 2010; Basu et al., 2007). These observations were interpreted as the formation of ferritin-PrP coaggregates, which confers both PrP resistance to PK digestion and detergent-insoluble characteristics (Basu et al., 2007; Singh et al., 2009;

Das et al., 2010). However, ferritin upregulation and the formation of PrP coaggregates occurred regardless of iron's cationic valence states (Das et al., 2010; Basu et al., 2007). Therefore, their explanation does not seem to account for the different outcomes we observed between Fe (II) and Fe (III) in this study. The discrepancies may be explained in at least 2 ways. First, there are distinctive molecular mechanisms of intracellular iron transport depending on iron's oxidative state: vesicular and nonvesicular iron import [30]. Cellular uptake of Fe (III) occurs via receptor-mediated endocytosis of transferrin (Tf). The Fe (III)-Tf complex then binds to a specific membrane-bound transferring receptor. Uptake of Fe (II), on the other hand, is mediated by plasma membrane-localized iron importers such as DMT1 and TRPML1. Vesicular transport of rPrP and Fe (III) might provide a favorable environment for PrP conversion. Second, Fe (II) and Fe (III) may have different binding affinities for rPrP. The affinity of PrP for iron is still unknown. Although limited to *in vitro* experiments with rPrP, Fe (III), and not Fe (II), was able to bind to rPrP (Brown et al., 2000; Basu et al., 2007). It is interesting to note that conversion of normal PrP to PrP^{Sc}-like characteristics is rPrP-specific, and not a general phenomenon, as shown here by the negligible changes in internalized rGal-3 levels regardless of Fe (III) exposure (Fig. 6). However, we cannot exclude the possibility that other neurodegenerative disease-associated proteins might also be affected by Fe (III).

The mechanism of conversion from rPrP to PrP^{res} remains unclear. However, the result from the cell-free reaction clearly demonstrates that Fe

(III)-mediated PrP^{res} conversion was induced not due to a direct contact between Fe (III) and rPrP, and instead requires a complex cellular milieu (Fig. 9). Moreover, we find that ROS is an auxiliary factor that participates in PrP conversion. Through the Fenton reaction, redox-active metals including iron and copper can promote generation of ROS, such as the hydroxyl radical derived from hydrogen peroxide (White et al., 1999). The involvement of ROS in the formation of PrP^{res} was supported by the inhibitory effect of DMSO in our experiments (Fig. 10). Redox-active iron in the vicinity of rPrP might increase the possibility of attack at sites in the proteins by generating free radicals, potentiating the PrP conversion process. However, the partial inhibitory effect of DMSO suggests that not only ROS but also other cellular factor(s) participate in the Fe (III)-mediated intracellular conversion.

Assessment of PK resistance after treatment with U18666A or NH_4Cl demonstrated that vesicular trafficking, and not acidic lysosomes is a relevant process/site where Fe (III)-associated PrP conversion occurred (Fig. 11 and 12). If conversion to PrP^{res} was because of the acidic environment in the lysosomes, under acidification inhibition, it would have been sensitive to PK treatment. This notion simply excludes the involvement of acidic lysosomes in the generation of Fe (III)-mediated PrP^{res}. Noticeably, reduction of PrP^{res} with U18666A indicated blockage of PrP^{res} formation. This suggests that endosomal trafficking may play a role in PrP^{res} formation. Since endocytosed and intracellular components within vesicles dynamically transit through homotypic and heterotypic membrane fusion along the

pathway leading to lysosomes (van der Goot and Gruenberg, 2006), a factor(s) present in vesicles might be required for the rPrP to obtain PK resistance. The observations that cholesterol depletion reduced PrP^{Sc} levels have underscored the importance of a lipid environment for PrP conversion (Bate et al., 2004; Mange et al., 2000). This phenomenon has been explained by the perturbation of PrP^{C} to associate with lipid rafts (Taraboulos et al., 1995), membrane microdomains characterized by a high content of sphingolipids and cholesterol, and the reduction of cell surface expression of PrP^{C} (Gilch et al., 2006). Although U18666A, which inhibits cholesterol recycling, has also been shown to impair PrP^{Sc} propagation, it did not affect the interaction between PrP^{C} and lipid rafts (Marijanovic et al., 2009; Gilch et al., 2009). Moreover, the HpL3-4 cell line is PrP^{C}-deficient, and therefore, the cell surface expression of PrP^{C} is required for neither U18666A-mediated PrP^{res} reduction nor Fe (III)-associated PrP^{res} generation in this experimental condition.

A limitation of this study is that cells were exposed to excessive amounts of iron compared to the levels found in diseased brains or other iron-overloaded cell models (Das et al., 2010; Basu et al., 2007). Despite the artificial condition, PrP^{res} in our experimental cell model exhibited PrP^{Sc}-like features including partial PK resistance and detergent insolubility; this presumably corresponds to the recombinant PrP^{res} that was converted by PrP^{Sc} in terms of biochemical properties and molecular size (Atarashi et al., 2008; Eiden et al., 2006). The cellular model shows similar phenomenon seen in PrP^{Sc}-infected cells including acquisition of PK resistance, an inhibitory effect of

U18666A on the generation of PrP^{res} (Goold et al., 2011), and maintenance of PK resistance following inhibition of lysosomal acidification (Marijanovic et al., 2009). Therefore, this experimental system can be a useful tool to study intracellular mechanism of PrP conversion, to evaluate potential drugs with anti-prion activity, and for assessment of the neurotoxic effects of PrP isoforms. Iron dyshomeostasis has been observed not only in prion-infected brains and animal models but also in sporadic prion disease (Singh et al., 2009; Caughey and Baron, 2006). Furthermore, not only normal aging brain but also brains with other neurodegenerative diseases, including Alzheimer's and Parkinson's (Mills et al., 2010), have shown abnormal iron accumulation. Therefore, this cell model can provide insight into the potential roles of iron in cognitive decline and its association with disease-specific proteins.

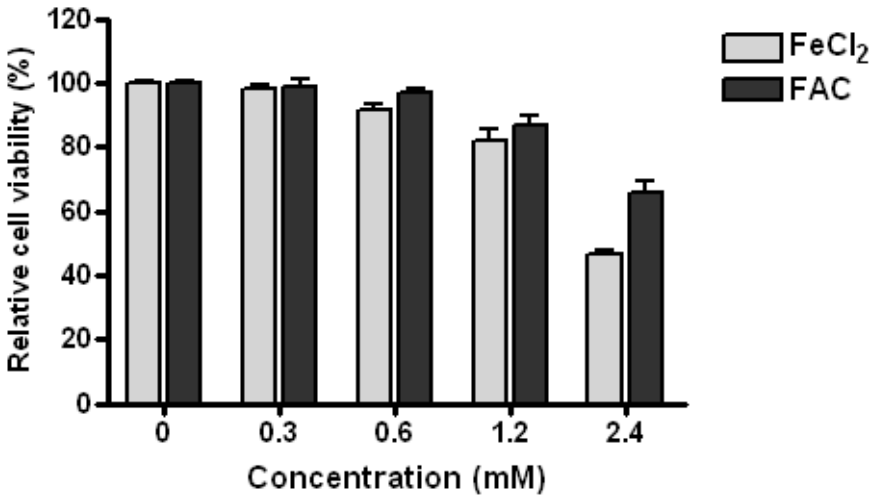

Figure 1. Cytotoxicity of iron in PrP^C deficient HpL3-4 cells.

Cell viability was assessed by CCK-8. Cells were exposed to $FeCl_2$ and FAC with various concentrations, and then incubated with 10 μL of WST-8 for another 4 h. The absorbance was measured at 450 nm, and the results are expressed as mean +/- STDV.

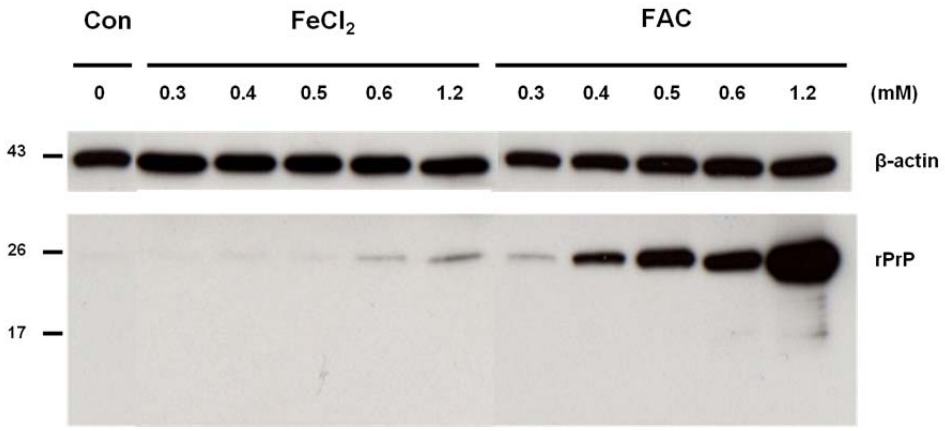

Figure 2. Concentration-dependent accumulation of internalized rPrP with Fe (III). The cells were exposed 0.3 to 1.2 mM $FeCl_2$ or FAC for 24 h. Then 0.6 μM rPrP was added and incubated for another 24 h. Equal amounts of cell lysate were resolved by performing SDS-PAGE and were immunoblotted. rPrP was detected by 1E4. β-actin was detected to be a loading control.

A

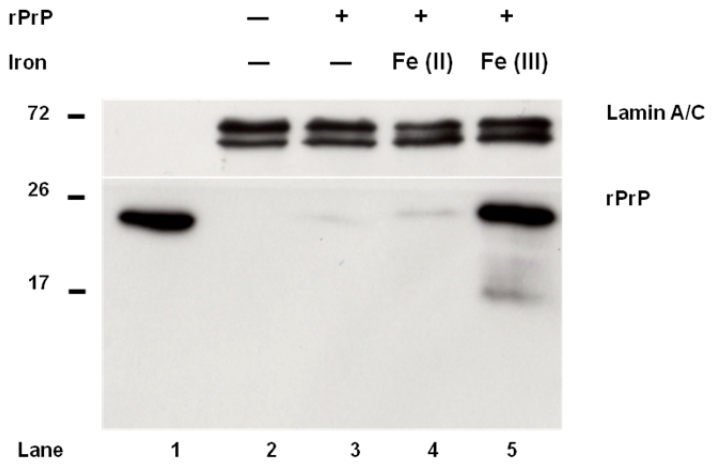
rPrP
—
+
+
+
Iron
—
—
Fe (II)
Fe (III)
72
26
17
Lamin A/C
rPrP
Lane
1
2
3
4
5

B

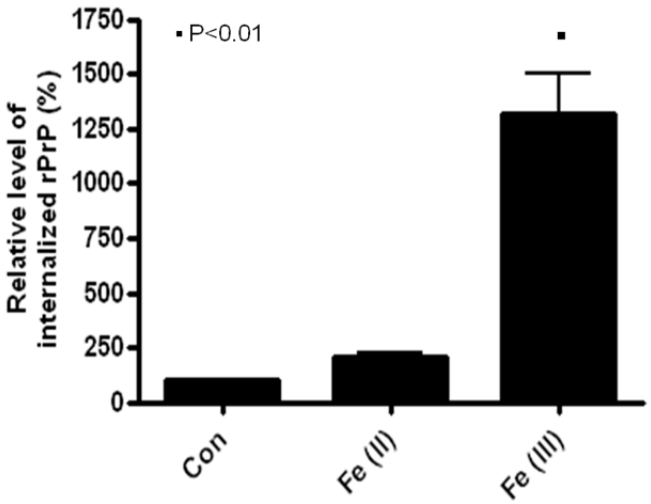
P<0.01
Relative level of internalized rPrP (%)
1750
1500
1250
1000
750
500
250
0
Con
Fe (II)
Fe (III)

Figure 3. Accumulation of internalized rPrP with Fe (III).

(A) Immunoblotting of internalized rPrP from mock- (lane 3), Fe (II)- (lane 4), or Fe (III)-(lane 5) exposed cell lysates with 1E4. No signal was detected from the cell lysates without rPrP treatment (lane 2). Purified rPrP (200 ng, lane 1) was loaded to compare the electrophoretic run of intact and fragmented PrP before and after intracellular uptake. (B) Quantification of internalized rPrP showed a dramatic increase (above 13-fold) in the level of rPrP from the cells exposed to Fe (III), unlike that observed in the control (Con). Levels of rPrP from each lysate were normalized to lamin A/C. Values are represented as percentage of rPrP level with iron exposures (mean +/-STDV) with respect to the control. Statistical significance between the experimental groups and control was shown as ($p < 0.01$).

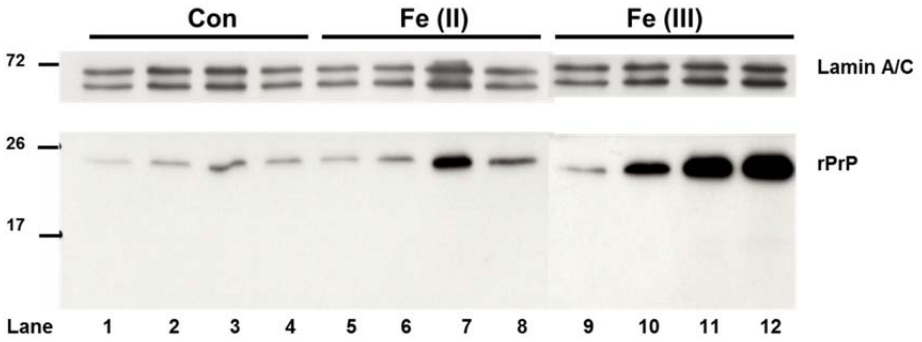

Figure 4. Time-dependent accumulation of internalized rPrP with Fe (III) exposure. Detection of rPrP from cells treated with rPrP for 4 (lane 1, 5, and 9), 8 (lane 2, 6, and 10), 16 (lane 3, 7, and 11), or 24 h (lane 4, 8, and 12) showed a time-dependent appearance of rPrP.

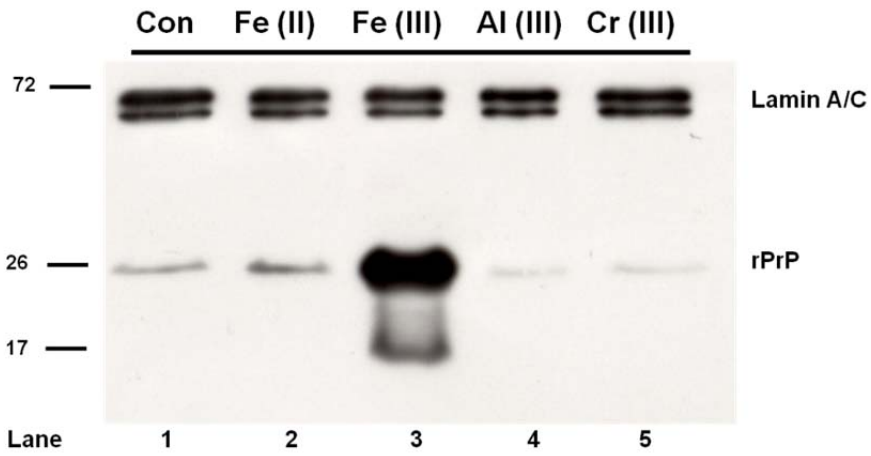

Figure 5. Fe (III)-specific accumulation of rPrP. The cells were exposed to other trivalent metal ions, Al (III) and Cr (III), as well as Fe (II) and Fe (III). Al (III) or Cr (III) did not induce an increase in the level of rPrP in the cells (lane 4 or 5).

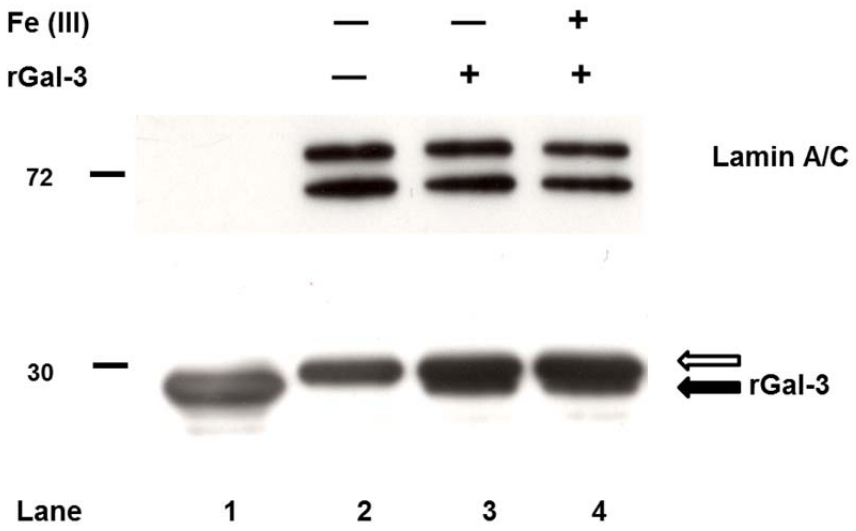

Figure 6. rPrP-specific accumulation with Fe (III). Immunoblotting of rGal-3 from the cells that were exposed to mock (lane 3) or Fe (III) (lane 4) for 24 h and then treated with 0.6 μM rGal-3 for another 24 h. Endogenous galectin-3 (white arrow) was detected from cells without rGal-3 treatment (lane 2). Purified rGal-3 (50 ng) was loaded to distinguish the internalized rGal-3 (black arrow) from the endogenous galectin-3 (lane 1).

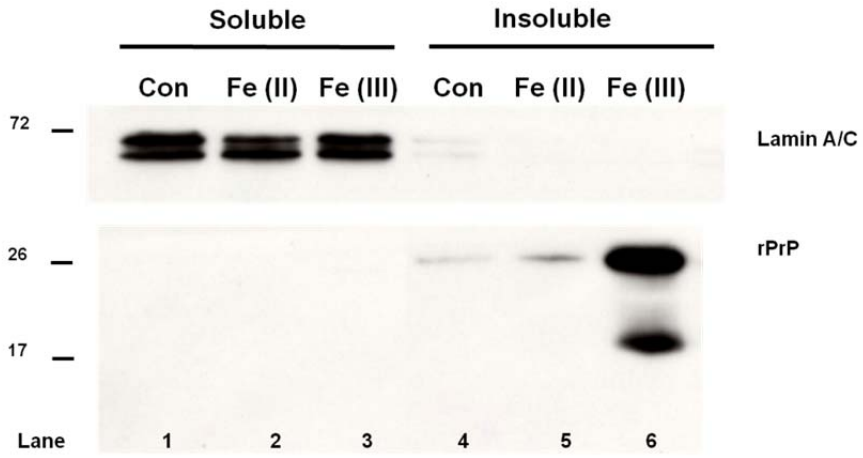

Figure 7. Insoluble rPrP in a detergent containing SDS. The cells were exposed to iron for 24 h and additionally treated with rPrP (0.6 μM) for another 24 h. Collected cells were lysed in 0.25 % SDS containing lysis buffer, cleared of debris, and pelleted. Supernatants (lane 1–3) and pellet (lane 4–6) were fractionated by performing SDS-PAGE and were immunoblotted.

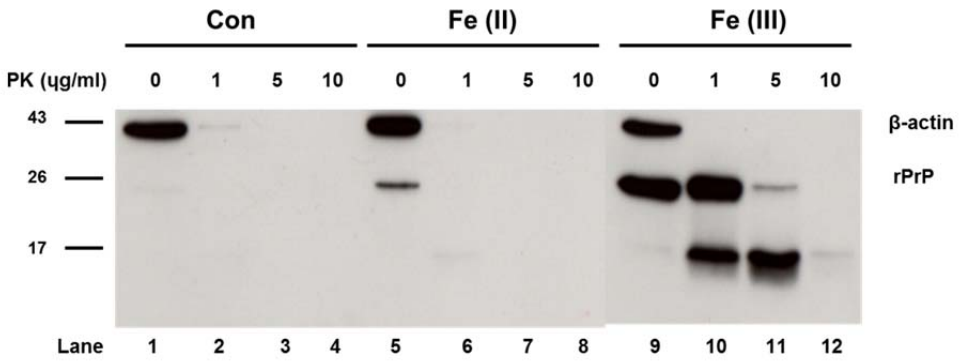

Figure 8. Conversion from rPrP to PrP^{res} with Fe (III). The cells exposed to iron for 24 h were treated with rPrP (0.6 μM) for another 24 h. Proteins from each cell lysate (1 mg/mL) were treated with PK (1, 5, and 10 μg/mL) for 30 min at 37°C. From the cells exposed to Fe (III), both intact (25 kDa) and fragment (16 kDa) were detected at 5 μg/mL PK, indicating that internalized rPrP acquired partial PK resistance (lane 11). At 10 μg/mL of PK, the majority of PrP were degraded but a weak signal from the PK-resistant fragment was detected (lane 12). On the contrary, rPrP from cells exposed to Fe (II) (lane 5–8) were completely degraded by PK at 1 μg/mL, which was similar to the observation for the mock-exposed cells (Con) (lane 1–4).

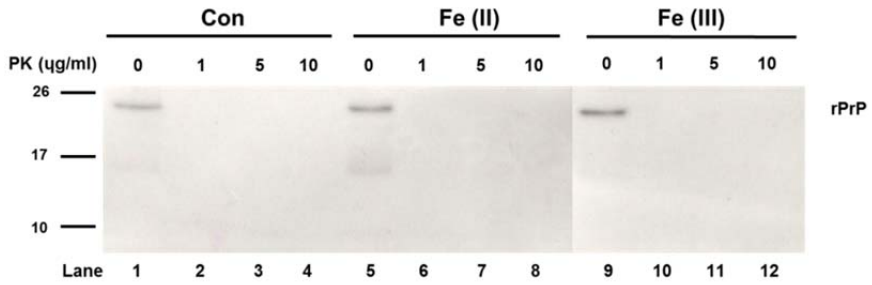

Figure 9. Failure to generate PrP^{res} in a cell free reaction. Iron and rPrP (0.6 μM in 20 mM HEPES, pH7.4) were allowed to react under cell-free conditions *in vitro*. rPrP exposed to mock, Fe (II), or Fe (III) at 37°C for 24 h showed a complete degradation by PK at 1 μg/mL.

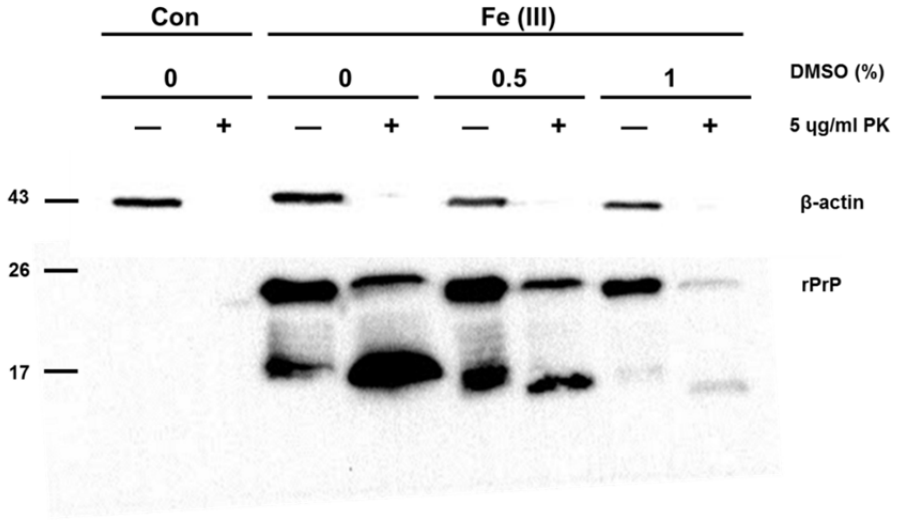

Figure 10. Partial involvement of ROS in the generation of PrP^{res}. Levels of rPrP (PK-) and PrP^{res} (PK+) after DMSO treatment were analyzed by immunoblotting. DMSO, a ROS scavenger, was added to cells 30 min prior to Fe (III) exposure. After 24 h incubation, 0.6 μM rPrP were then added to media for another 24 h. The collected cells in the lysis buffer without protease inhibitors were incubated with PK.

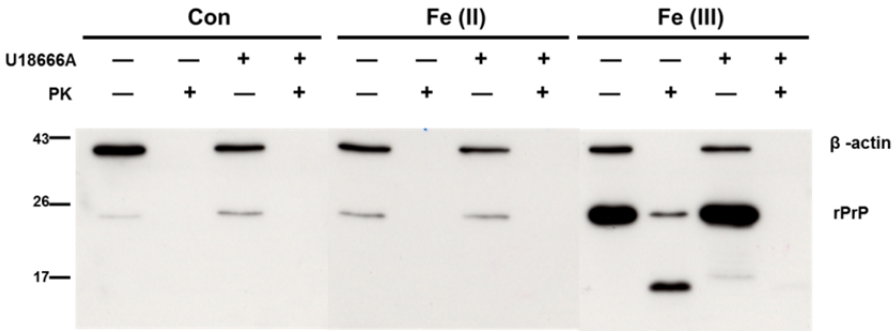

Figure 11. Inhibition of PrP^{res} generation by U18666A. Levels of rPrP (PK-) and PrP^{res} (PK+) after U18666A treatment were analyzed by immunoblotting. Cells exposed to mock, Fe (II), or Fe (III) were treated with (+) or without (-) 3 μM U18666A for 24 h (A). Then 0.6 μM rPrP was treated with the media for another 24 h. The lysates were incubated with PK at 5 μg/mL (PK+) or were left untreated (PK-). Following U18666A treatment, the formation of PrP^{res} decreased.

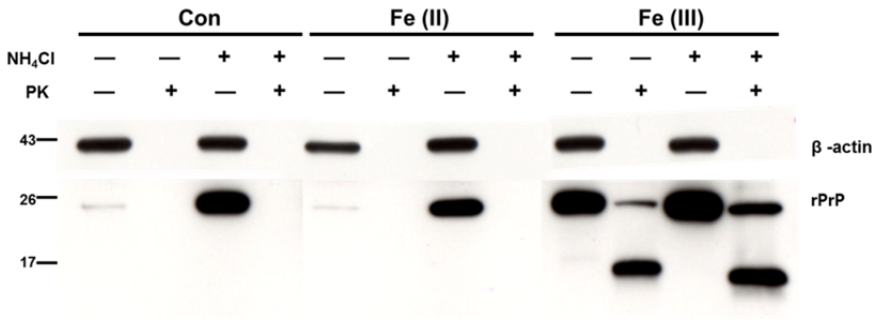

Figure 12. No effect of NH_4Cl on PrP^{res} generation. Levels of rPrP (PK-) and PrP^{res} (PK+) after NH_4Cl treatment were analyzed by immunoblotting. Cells exposed to mock, Fe (II), or Fe (III) were treated with (+) or without 20 mM NH_4Cl. Then 0.6 μM rPrP was added to the media for another 24 h. Lysates were incubated with PK at 5 μg/mL (PK+) or were left untreated (PK-). NH_4Cl treatment did not affect the generation of PrP^{res}.

V. References

Alais, S., S. Simoes, D. Baas, S. Lehmann, G. Raposo, J. L. Darlix, and P. Leblanc. 2008. Mouse neuroblastoma cells release prion infectivity associated with exosomal vesicles. *Biol Cell* 100 (10):603-15.

Atarashi, R., J. M. Wilham, L. Christensen, A. G. Hughson, R. A. Moore, L. M. Johnson, H. A. Onwubiko, S. A. Priola, and B. Caughey. 2008. Simplified ultrasensitive prion detection by recombinant PrP conversion with shaking. *Nat Methods* 5 (3):211-2.

Basu, S., M. L. Mohan, X. Luo, B. Kundu, Q. Kong, and N. Singh. 2007. Modulation of proteinase K-resistant prion protein in cells and infectious brain homogenate by redox iron: implications for prion replication and disease pathogenesis. *Mol Biol Cell* 18 (9):3302-12.

Bate, C., M. Salmona, L. Diomede, and A. Williams. 2004. Squalestatin cures prion-infected neurons and protects against prion neurotoxicity. *J Biol Chem* 279 (15):14983-90.

Brown, D. R., F. Hafiz, L. L. Glasssmith, B. S. Wong, I. M. Jones, C. Clive, and S. J. Haswell. 2000. Consequences of manganese replacement of copper for prion protein function and proteinase resistance. *EMBO J* 19 (6):1180-6.

Brown, L. R., and D. A. Harris. 2003. Copper and zinc cause delivery of the prion protein from the plasma membrane to a subset of early endosomes and the Golgi. *J Neurochem* 87 (2):353-63.

Caughey, B., and G. S. Baron. 2006. Prions and their partners in crime. *Nature* 443 (7113):803-10.

Cenedella, R. J. 2009. Cholesterol synthesis inhibitor U18666A and the role of sterol metabolism and trafficking in numerous pathophysiological processes. *Lipids* 44 (6):477-87.

Collinge, J. 2001. Prion diseases of humans and animals: their causes and molecular basis. *Annu Rev Neurosci* 24:519-50.

Das, D., X. Luo, A. Singh, Y. Gu, S. Ghosh, C. K. Mukhopadhyay, S. G. Chen, M. S. Sy, Q. Kong, and N. Singh. 2010. Paradoxical role of prion protein aggregates in redox-iron induced toxicity. *PLoS One* 5 (7):e11420.

Eiden, M., G. J. Palm, W. Hinrichs, U. Matthey, R. Zahn, and M. H. Groschup. 2006. Synergistic and strain-specific effects of bovine spongiform encephalopathy and scrapie prions in the cell-free conversion of recombinant prion protein. *J Gen Virol* 87 (Pt 12):3753-61.

Fernaeus, S., and T. Land. 2005. Increased iron-induced oxidative stress and toxicity in scrapie-infected neuroblastoma cells. *Neurosci Lett* 382 (3):217-20.

Gilch, S., C. Bach, G. Lutzny, I. Vorberg, and H. M. Schatzl. 2009. Inhibition of cholesterol recycling impairs cellular PrP(Sc) propagation. *Cell Mol Life Sci* 66 (24):3979-91.

Gilch, S., C. Kehler, and H. M. Schatzl. 2006. The prion protein requires cholesterol for cell surface localization. *Mol Cell Neurosci* 31 (2):346-53.

Goold, R., S. Rabbanian, L. Sutton, R. Andre, P. Arora, J. Moonga, A. R. Clarke, G. Schiavo, P. Jat, J. Collinge, and S. J. Tabrizi. 2011. Rapid cell-surface prion protein conversion revealed using a novel cell system. *Nat Commun* 2:281.

Jackson, G. S., L. L. Hosszu, A. Power, A. F. Hill, J. Kenney, H. Saibil, C. J. Craven, J. P. Waltho, A. R. Clarke, and J. Collinge. 1999. Reversible conversion of monomeric human prion protein between native and fibrilogenic conformations. *Science* 283 (5409):1935-7.

Kaul, S., A. Kanthasamy, M. Kitazawa, V. Anantharam, and A. G. Kanthasamy. 2003. Caspase-3 dependent proteolytic activation of protein kinase C delta mediates and regulates 1-methyl-4-phenylpyridinium (MPP+)-induced apoptotic cell death in dopaminergic cells: relevance to oxidative stress in dopaminergic degeneration. *Eur J Neurosci* 18 (6):1387-401.

Kim, B. H., Y. C. Jun, J. K. Jin, J. I. Kim, N. H. Kim, E. A. Leibold, J. R. Connor, E. K. Choi, R. I. Carp, and Y. S. Kim. 2007. Alteration of iron regulatory proteins (IRP1 and IRP2) and ferritin in the brains of scrapie-infected mice. *Neurosci Lett* 422 (3):158-63.

Kim, N. H., S. J. Park, J. K. Jin, M. S. Kwon, E. K. Choi, R. I. Carp, and Y. S. Kim. 2000. Increased ferric iron content and iron-induced oxidative stress in the brains of scrapie-infected mice. *Brain Res* 884 (1--2):98-103.

Kobayashi, T., M. H. Beuchat, M. Lindsay, S. Frias, R. D. Palmiter, H. Sakuraba, R. G. Parton, and J. Gruenberg. 1999. Late endosomal membranes rich in lysobisphosphatidic acid regulate cholesterol transport. *Nat Cell Biol* 1 (2):113-8.

Kuwahara, C., A. M. Takeuchi, T. Nishimura, K. Haraguchi, A. Kubosaki, Y. Matsumoto, K. Saeki, T. Yokoyama, S. Itohara, and T. Onodera. 1999. Prions prevent neuronal cell-line death. *Nature* 400 (6741):225-6.

Mange, A., N. Nishida, O. Milhavet, H. E. McMahon, D. Casanova, and S. Lehmann. 2000. Amphotericin B inhibits the generation of the scrapie isoform of the prion protein in infected cultures. *J Virol* 74 (7):3135-40.

Marijanovic, Z., A. Caputo, V. Campana, and C. Zurzolo. 2009. Identification of an intracellular site of prion conversion. *PLoS Pathog* 5 (5):e1000426.

Martins, S. M., D. J. Frosoni, A. M. Martinez, F. G. De Felice, and S. T. Ferreira. 2006. Formation of soluble oligomers and amyloid fibrils with physical properties of the scrapie isoform of the prion protein from the C-terminal domain of recombinant murine prion protein mPrP-(121-231). *J Biol Chem* 281 (36):26121-8.

Mayran, N., R. G. Parton, and J. Gruenberg. 2003. Annexin II regulates multivesicular endosome biogenesis in the degradation pathway of animal cells. *EMBO J* 22 (13):3242-53.

Milhavet, O., H. E. McMahon, W. Rachidi, N. Nishida, S. Katamine, A. Mange, M. Arlotto, D. Casanova, J. Riondel, A. Favier, and S. Lehmann. 2000. Prion infection impairs the cellular response to oxidative stress. *Proc Natl Acad Sci U S A* 97 (25):13937-42.

Mills, E., X. P. Dong, F. Wang, and H. Xu. 2010. Mechanisms of brain iron transport: insight into neurodegeneration and CNS disorders. *Future Med Chem* 2 (1):51-64.

Pauly, P. C., and D. A. Harris. 1998. Copper stimulates endocytosis of the prion protein. *J Biol Chem* 273 (50):33107-10.

Petersen, R. B., S. L. Siedlak, H. G. Lee, Y. S. Kim, A. Nunomura, F. Tagliavini, B. Ghetti, P. Cras, P. I. Moreira, R. J. Castellani, M. Guentchev, H. Budka, J. W. Ironside, P. Gambetti, M. A. Smith, and G. Perry. 2005. Redox metals and oxidative abnormalities in human prion diseases. *Acta Neuropathol* 110 (3):232-8.

Qin, K., D. S. Yang, Y. Yang, M. A. Chishti, L. J. Meng, H. A. Kretzschmar, C. M. Yip, P. E. Fraser, and D. Westaway. 2000. Copper(II)-induced conformational changes and protease resistance in recombinant and cellular PrP. Effect of protein age and deamidation. *J Biol Chem* 275 (25):19121-31.

Rana, A., D. Gnaneswari, S. Bansal, and B. Kundu. 2009. Prion metal interaction: is prion pathogenesis a cause or a consequence of metal imbalance? *Chem Biol Interact* 181 (3):282-91.

Singh, A., A. O. Isaac, X. Luo, M. L. Mohan, M. L. Cohen, F. Chen, Q. Kong, J. Bartz, and N. Singh. 2009. Abnormal brain iron homeostasis in human and animal prion disorders. *PLoS Pathog* 5 (3):e1000336.

Singh, A., M. L. Mohan, A. O. Isaac, X. Luo, J. Petrak, D. Vyoral, and N. Singh. 2009. Prion protein modulates cellular iron uptake: a novel function with implications for prion disease pathogenesis. *PLoS One* 4 (2):e4468.

Singh, N., D. Das, A. Singh, and M. L. Mohan. 2009. Prion Protein and Metal Interaction: Physiological and Pathological Implications. *Curr Issues Mol Biol* 12 (2):99-108.

Singh, N., A. Singh, D. Das, and M. L. Mohan. 2010. Redox control of prion and disease pathogenesis. *Antioxid Redox Signal* 12 (11):1271-94.

Taraboulos, A., M. Scott, A. Semenov, D. Avrahami, L. Laszlo, and S. B. Prusiner. 1995. Cholesterol depletion and modification of COOH-terminal targeting sequence of the prion protein inhibit formation of the scrapie isoform. *J Cell Biol* 129 (1):121-32.

Thackray, A. M., R. Knight, S. J. Haswell, R. Bujdoso, and D. R. Brown. 2002.

Metal imbalance and compromised antioxidant function are early changes in prion disease. *Biochem J* 362 (Pt 1):253-8.

Thellung, S., A. Corsaro, V. Villa, A. Simi, S. Vella, A. Pagano, and T. Florio. 2011. Human PrP90-231-induced cell death is associated with intracellular accumulation of insoluble and protease-resistant macroaggregates and lysosomal dysfunction. *Cell Death Dis* 2:e138.

van der Goot, F. G., and J. Gruenberg. 2006. Intra-endosomal membrane traffic. *Trends Cell Biol* 16 (10):514-21.

Watt, N. T., D. R. Taylor, A. Gillott, D. A. Thomas, W. S. Perera, and N. M. Hooper. 2005. Reactive oxygen species-mediated beta-cleavage of the prion protein in the cellular response to oxidative stress. *J Biol Chem* 280 (43):35914-21.

Westergard, L., H. M. Christensen, and D. A. Harris. 2007. The cellular prion protein (PrP(C)): its physiological function and role in disease. *Biochim Biophys Acta* 1772 (6):629-44.

White, A. R., S. J. Collins, F. Maher, M. F. Jobling, L. R. Stewart, J. M. Thyer, K. Beyreuther, C. L. Masters, and R. Cappai. 1999. Prion protein-deficient neurons reveal lower glutathione reductase activity and increased susceptibility to hydrogen peroxide toxicity. *Am J Pathol* 155 (5):1723-30.

Zhou, M., G. Ottenberg, G. F. Sferrazza, and C. I. Lasmezas. 2012. Highly neurotoxic monomeric alpha-helical prion protein. *Proc Natl Acad Sci U S A* 109 (8):3113-8.

국문 초록

프리온 질병은 단백질 변성에 기인하는 퇴행성 뇌질병 중의 하나이다. 이 질병의 주요 현상인 프리온 단백질의 응집과 신경독성은 전염성을 지닌 병원성 단백질의 축적에 의한 결과라고 생각되어 지고 있다. 하지만 병원성 프리온 이외에 다른 요인들도 프리온 변성에 영향을 줄 수 있음이 제기된 바 있다. 정상 프리온 단백질의 생리적인 기능은 명확히 밝혀지진 않았지만 금속 이온의 항상성 조절에 관여함이 보고되어 있다. 특히, 프리온 질병에서 철 이온의 증가가 관찰되는데 이는 프리온 단백질이 철 저장체와 응집을 이루기 때문으로 여겨진다. 철 이온이 변성 프리온 생성에 관련되어 있음이 보고되어 있다. 이 학위논문에서는 이온가에 따른 철이 프리온 변성에 어떠한 영향을 미치는지와 이에 관한 메커니즘을 다룬다. 본 실험은 프리온 단백질을 발현하지 않는 세포(HpL3-4)에 이가철 또는 삼가철을 노출한 후 재조합 프리온 단백질을 외부에서 처리하였다. 이에 따라 세포로 유입되어 존재하는 프리온의 양을 확인하여 보고 이의 생화학적 성질 변화를 알아보기 위하여 proteinase K (PK) 분해에 대한 저항성과 detergent 불용성을 살펴보았다. U18666A와 NH_4Cl을 각각 사용하여 소포성 운반과정과 소포-리소좀의 산성화를 저해해 봄으로써 프리온 단백질 변성이 일어나는 과정을 유추하여보았다. 실험을 통하여 이가철이 아닌 삼가철 특이적으로 세포 내 프리온 단백질의 축적을 확인하였으며 이는 철의 농도와 프리온 단백질의

처리 시간에 현격히 비례함을 확인할 수 있었다. 또한 이러한 단백질의 축적은 galectin-3를 처리시 나타나지 않음을 통하여 프리온 특이적인 반응인 것으로 판단할 수 있었다. 삼가철에 의해 축적된 프리온 단백질은 detergent에 불용성을 띄었으며 PK 분해에 저항성을 띄는 PrP^{res} 이었다. 뿐만 아니라, 변성 프리온의 생성은 U18666A에 의해서 저해되었으며 NH_4Cl에 의한 영향은 없었다. 이를 통하여 삼가철 매개의 변성 프리온 생성은 리소좀의 산성환경이 아닌 소포성 운반 과정에서 형성된 것을 유추할 수 있었다. 이제까지의 실험을 통하여 이가철 보다 삼가철이 프리온의 변성에 관여하며 이러한 변성은 소포성의 운반과정에서 발생할 것으로 보인다.

주요어 : 철 이온, 재조합 프리온 단백질, 변성, PrP^{res}, 소포성 운반, 리소좀
학번 : 2009-21645